

# Plant Extraction and Physicochemical Characterizations of Untreated and Pretreated Diss Fibers (*Ampelodesmos mauritanicus*)

Mustapha Nouri, Ismail Griballah, Mahfoud Tahlaiti, Frederic Grondin,  
Johnny Beaugrand

► **To cite this version:**

Mustapha Nouri, Ismail Griballah, Mahfoud Tahlaiti, Frederic Grondin, Johnny Beaugrand. Plant Extraction and Physicochemical Characterizations of Untreated and Pretreated Diss Fibers (*Ampelodesmos mauritanicus*). *Journal of Natural Fibers*, Taylor & Francis, 2019, pp.1-11. 10.1080/15440478.2019.1687062 . hal-03142112

**HAL Id: hal-03142112**

**<https://hal.inrae.fr/hal-03142112>**

Submitted on 6 May 2021

**HAL** is a multi-disciplinary open access archive for the deposit and dissemination of scientific research documents, whether they are published or not. The documents may come from teaching and research institutions in France or abroad, or from public or private research centers.

L'archive ouverte pluridisciplinaire **HAL**, est destinée au dépôt et à la diffusion de documents scientifiques de niveau recherche, publiés ou non, émanant des établissements d'enseignement et de recherche français ou étrangers, des laboratoires publics ou privés.



# Plant Extraction and Physicochemical Characterizations of Untreated and Pretreated Diss Fibers (*Ampelodesmos mauritanicus*)

Mustapha Nouri<sup>a,b</sup>, Ismail Griballah<sup>a</sup>, Mahfoud Tahlaiti<sup>a,b</sup>, Frédéric Grondin<sup>b</sup>, and Johnny Beaugrand<sup>c</sup>

<sup>a</sup>Institut Catholique d'Arts et Métiers, Carquefou, France; <sup>b</sup>Institut de Recherche en Génie Civil et Mécanique (GeM), UMR 6183, Centrale de Nantes - Université de Nantes - CNRS, Nantes, France; <sup>c</sup>Biopolymères Interactions Assemblages (BIA), INRA, Nantes, France

## ABSTRACT

The *Ampelodesmos mauritanicus* plant, *Mauritanian grass* or also called 'Diss', is a perennial abundant plant on the Mediterranean contour, having attractive characteristics for ecofriendly materials. This work aims to highlight the potential of the Diss fibers elements by assessing their use as reinforcement for polymer matrices (bio-composite). So, untreated and treated Diss fibers by chemical (soda, silane and acetic acid) and thermal treatment have been manually extracted and characterized to evaluate their surface condition as well as their chemical composition, their mechanical properties and their thermal stability. The obtained results have shown many advantages look promising for such an application, especially the fact that the Diss fiber bundles has small diameter ( $89 \pm 22 \mu\text{m}$ ), a rough surface with the presence of thorns, a low density of  $0.93 \text{ g/cm}^3$ , and a tensile strength that can reach 270 MPa. Furthermore, all the treatments adopted have shown improvements regarding the fibrillation of fiber bundles (could reach  $-40\%$  for the diameter), their surface state, their thermal stability and their mechanical behavior (could reach  $+60\%$  for Young's modulus and  $+15\%$  for tensile stress).

## Introduction

The depletion of resources and global warming have pushed all industries to adopt a green and more sustainable production. In the field of composites, one of these movements consists in substituting the synthetic materials, such as carbon and glass fibers, by other natural substances holding less environmental impact, such as cellulosic fibers. To the fact that they are biodegradable, these fibers present an ecological

interest, because they appear to be neutral in terms of CO<sub>2</sub> emissions in the atmosphere (Baley 2013). Furthermore, other benefits of these fibers can be mentioned such as their low cost and the fact that they are renewable resources.

Currently, Despite the wide range of plants already exploited in the world, there is still a vast variety of plants not yet sufficiently studied such as the Diss plant. Mauritanian grass, Diss, or *Ampelodesmos mauritanicus*, is a plant species of the family Poaceae (Damerdji 2012). This herbaceous perennial plant can reach two to three meters high, is rich in fibers, robust with acuminate leaves and it grows as tufts in more or less dry soils (Damerdji 2012; Rameau, Mansion, and Dumé 1989). Diss is one of the most abundant plant resources in the Mediterranean contour (Achour, Ghomari, and Belayachi 2017). It was formerly used to build the roofs of old houses thanks to their mechanical and hydrous qualities (Bourahli 2014). The exploitation of these wild plant fibers as a reinforcement to cementitious composites is little studied in the literature and rarely studied for polymer composites.

Merzoud and Habita (2008) made a composite from crushed Diss fibers and cement matrix. Recently, Bourahli and Osmani (2013) have carried out an in-depth study of Diss fibers in which their chemical compositions and the tensile strength were determined. Furthermore, Bourahli (2014) found that the incorporation of Diss fibers into a polyester matrix led to an improvement of the matrix mechanical properties. Lately, Achour, Ghomari, and Belayachi (2017) investigated the effect of various treatments and the fibers loading rate on the physical, mechanical and thermal properties of the composite Diss fibers/cement. Very recently, Sarasini et al. (2019) studied the reinforcement of PP and PLA matrix by Diss fibers.

However, to this day, there is no extraction method dedicated to this type of plant, which should take into account its particular morphology comparing to other plants. Generally, the extraction procedure occurs on an industrial scale mechanically. The lack of a suitable extraction technique for this type of plant, as was observe in the literature, make its industrial exploitation difficult. Merzoud and Habita (2008) crushed the diss plant to have, what they call, diss fibers. Bourahli (2014) used during his thesis dissolutions by retting and soda. Sarasini et al. (2019) used an enzymatic method. In addition, the extraction method clearly influences the mechanical properties of the fibers. Bourahli (2014) found an average tensile stresses of  $149 \pm 81$ , while Sarasini et al. (2019) found a low one of 19 MPa.

Although, the interface state between the fibers and the matrix plays a leading role in the stresses transmission in the polymer composite. Natural fibers contain free hydroxyl groups on their surface, coming from hemicellulose, pectin and cellulose to a lower extent, which produces their hydrophilic nature, while most polymer matrices are hydrophobic (Chilali 2017, Methacanon et al. 2010). To overcome this incompatibility, vegetal fibers are generally subjected to specific treatments, which may be mechanical, chemical, enzymatic or physical (Methacanon et al. 2010). Chemical treatments are the most widely adopted for vegetal fibers in the literature. In addition, physical treatments, such as heat treatment, are more responsible to the environment.

The purpose of this work is to characterize Diss plant and its fibers and optimize a treatment of these last in order to promote their use as reinforcements for polymer composites. We propose to fill a gap in the literature by investigating the diss plant fibers extraction and subsequent fibers thereof. Furthermore, several treatments have been studied on this kind of fibers: soda, silane, acetic acid and heat treatment from manually extracted Diss fibers. These treatments are intended to modify the surface of these fibers in order to obtain a good interfacial bond with the polymer matrix

## **Materials and methods**

### ***Diss fibers extraction***

The Diss plant leaves (Figure 1) were harvested by hand in the north of Algeria at the end of their maturity (in 2018). The manual extraction method was conducted as follows: First, retting the leaves with water for 11 days. Next, scraping the wet leaves using a cutting tool by fixing them on a rigid plate, this step produces fibers ribbons. Then, carding the fiber ribbons with two combs, this step



Figure 1. Diss plant.

produces the untreated Technical Fiber of Diss (UTFD). Finally, spreading the UTFD (about 50 mm long) and drying them at room temperature.

### ***Fiber surface treatment***

The thermal treatment of UTFD was carried out in an oven at a temperature of 140°C during 14h. Then, the thermally treated TFD (TTFD) were cooled down at room temperature. The temperature of the treatment was deduced from the work of Ariawan et al. (2018) concerning kenaf fibers.

The UTFD were submerged in an aqueous solution containing 5% NaOH at room temperature during 5h. Afterward the TFD treated with NaOH (NTFD) were first cleaned by immersing them in distilled water for 24h. They were then submerged in a solution of distilled water containing 2% of acetic acid in order to adjust the pH to 7. The pH degree was measured by a pH paper indicator. Finally, the NTFD were washed several times with tap water and dried in the oven at 60°C for 3h.

The UTFD were immersed in an acetic acid solution at room temperature during 90 min. Then, the acetylated TFD (ATFD) were treated with an ethyl acetate solution containing two drops of sulfuric acid to remove excess of acetic acid. Finally, the ATFD were cleaned with tap water and dried in the oven at 40°C for 24h. This protocol was inspired by the work of Haque et al. (2015).

Octyltriethoxysilane (2%) was dissolved in a mixture of distilled water/ethanol with a volume ratio of (0.40/0.60), respectively. This solution was adjusted using acetic acid until the pH value equalled 4, then the solution was stirred for 2h. Afterward, the UTFD were submerged in the solution for 2h at room temperature. Finally, the Silane-treated TFD (STFD) were cleaned with tap water and dried in the oven at 60°C for 3h.

### ***Fibers characterization***

#### ***Density measurement***

The density of the UTFD was measured by Pycnometer method. Three measurements were carried out using a volumetric flask of 100 cm<sup>3</sup>. The UTFD were cut in short length (about 5 mm) and then dried for 48h in a desiccator containing silica. For each measurement, one gram of fiber was introduced into the flask and then submerged with canola oil till the gauge mark. Before making the weighing, the UTFD were left in this state for 24h in order to let the microbubbles between the UTFD evacuate. Subsequently, the weighings were carried out for each sample using a Sartorius scale (1/1000). The apparent density was determined by equation (1).

$$\rho_f = \frac{m_f}{100 - \left(\frac{m_h}{\rho_h}\right)} \quad (1)$$

$\rho_f$ : Fiber density (g/cm<sup>3</sup>).  $\rho_h$ : Canola oil density (0.914 g/cm<sup>3</sup>).  $m_f$ : UTFDmass (g).  $m_h$ : canola oil mass of (g).

### **Microscopy**

An optical microscope (Infinity 2 – Olympus BH2) was used to observe the Diss leaves and UTFD cross-sections. The latter were measured using an image processing software (Infinity 2–3). The average diameter was determined after measuring at least 25 fibers bundles for each treatment. The section was presumed circular. The fiber bundles were coated in a cold-coating resin (versoCit-2). The leaves were included in LR-White Added resin (without fixation and without prior dehydration) then cut in 1  $\mu$ m slices using a microtome equipped with a diamond knife. The sections were subsequently treated with orange Acridine (0.02% diluted in 0.1M sodium phosphate buffer at pH = 7.20).

Treated and untreated TFD were also observed using a scanning electron microscope JEOL 6060 LA operating at 45 kV.

### **Chemical analysis**

Before determining their biochemical composition, Diss leaves and UTFD were milled separately with liquid nitrogen (N<sub>2</sub>) in a centrifugal grinding mill equipped with a 0.5 mm sieve (Retsh ZM100). Thereafter, carbohydrates and lignin, expressed as the percentage of the dry matter mass, were identified and quantified following the chromatographic method and the acetyl bromide method (Hatfield and Fukushima 2005), respectively. The amount of ash was determined after calcining the UTFD and Diss leaves in an oven at 900°C for 10h. All analyzes were performed in three independent assays. The chemicals were laboratory grade, obtained from Sigma Aldrich.

For the chromatographic method, 3g of samples were subjected to hydrolysis in 12 M H<sub>2</sub>SO<sub>4</sub> for 2 h at 25°C followed by additional hydrolysis of 2 h at 100°C with 1.5 M H<sub>2</sub>SO<sub>4</sub> in presence of inositol as internal standard. Galacturonic Acid (GalA) was determined by an automated m-hydroxybiphenyl method (Thibault 1979) whereas individual neutral sugars (arabinose, glucose, xylose and galactose) were analyzed as their alditol acetate derivatives (Blakeney, Harris, and Henry 1983) by gas-liquid chromatography (Perkin Elmer, Clarus 580, Shelton, CT, USA) equipped with an DB 225 capillary column (J&W Scientific, Folsom, CA, USA) at 205°C, with H<sub>2</sub> as the carrier gas.

### **Fourier transform infrared spectroscopy (FTIR)**

FTIR analysis of the TFD was performed with a Perkin Elmer spectrometer using transmission techniques. The spectra were recorded in the range of infrared rays from 4000 cm<sup>-1</sup> to 450 cm<sup>-1</sup>. The untreated and treated TFD were crushed into small particles and then mixed and pressed down with potassium bromide (KBr) into thin pellets.

### **Thermal analysis**

Thermogravimetric analysis (TG-DTG) of treated and untreated Diss fibers were performed using a Simultaneous Thermal Analyzer (NETZSCH STA 449 F3 Jupite). All measurements were taken by maintaining a constant heating rate of 20°C/min in an open ceramic crucible. The weight of the samples was about 40 mg, with a temperature range of 25 to 500°C.

### **Tensile test**

The tensile properties of Diss fiber bundles were obtained using an Instron universal tensile tester (Instron model 3366) provided with a load cell of 5 N. The tests were carried out under ambient temperature T  $\approx$  25°C and a relative humidity between 55 and 65%. The gauge length and the speed of the moving cross member were chosen in accordance with the standard NF T25-501-3, of 10 mm and

1 mm/min, respectively. Ten samples were tested for each treatment and the section was determined according to the method of Hu et al. (2010). The results were evaluated using the Dixon test (1953).

## Results and discussion

### *The density and the morphology of the Diss leaf*

The measured density of UTFD was  $0.93 \pm 0.01 \text{ g/cm}^3$ , similar to the value found by Bourahli and Osmani (2013);  $0.89 \text{ g/cm}^3$ . These UTFD have a rather low density compared to that of flax ( $1.53\text{--}1.54 \text{ g/cm}^3$ ), hemp ( $1.4\text{--}1.6 \text{ g/cm}^3$ ), sisal ( $1.45 \text{ g/cm}^3$ ) and Jute ( $1.38\text{--}1.40 \text{ g/cm}^3$ ) (Bourmaud et al. 2018).

The Diss plant has long leaves that fold it selves inwards after the harvest. Figure 2a highlights the cross-section of Diss leaves. Each one of these leaves has an approximate hundred micrometers of thickness. They are characterized by a smooth outer surface and an extremely undulated thorny inner surface (Figure 2b). The optical microscope observations of this leaf revealed that it is rich in fiber. Diss leaves are built from the outside toward the inside, as shown in Figure 2b, by a thick layer of outer epidermis, conductive (vascular) bundles in the middle surrounded by chlorophyll parenchyma and a thinner layer of inner epidermis that contains thorns (trichomes). The inner area of this leaf is filled with sclerenchyma cells, commonly known as “elementary fibers”.

### *Morphology of technical Diss fibers (TFD)*

Figure 3 illustrates the optical microscope observations on the cross-sections of TFD. These are often presented in a form of more or less thick ribbons. In addition, these TFDs are frequently connected to a part of the inner thorny epidermis and take its shape.

Figure 4 illustrates the average diameters of the treated and untreated TFD. UTFD had an average diameter of  $89 \pm 22 \mu\text{m}$ . However, a decrease of the average diameter of the treated TFD was observed: it reach 40%, 36%, 34%, 20% after NaOH, acetylation, silane and thermal treatments, respectively. Taking into account the uncertainty, this decrease in diameter becomes significant only

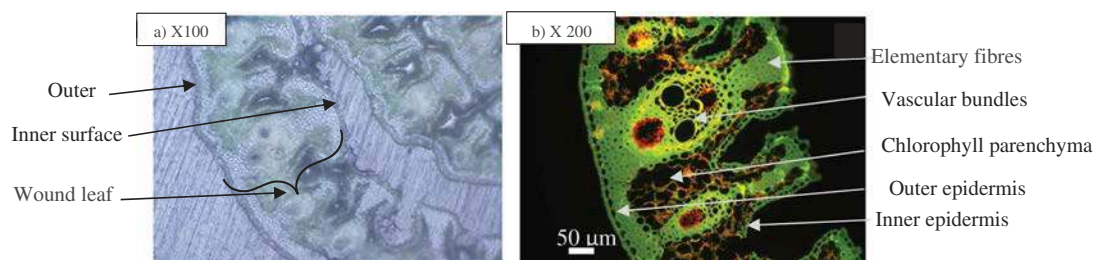


Figure 2. Observation of Diss leaves cross section by optical microscope (a) X100, (b) X200. (b) are treated with Acridine orange.

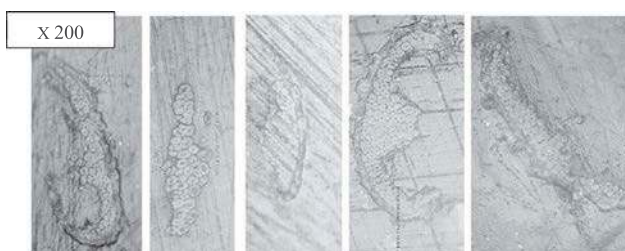


Figure 3. Observation by optical microscope of the cross section of UTFD.

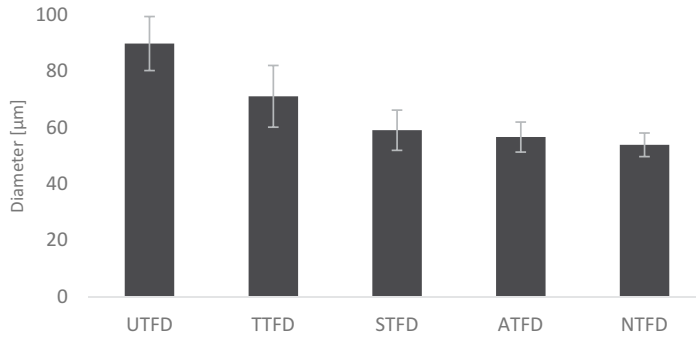


Figure 4. Variation of diameters of treated and untreated TFD, uncertainty ( $k = 2$ ).

after the chemical treatment. This could be due to the removal/degradation of some of the amount of natural cement that binds the individual fibers between them (middle lamella), which has caused the fibrillation of TFDs.

Figure 5 shows SEM pictures of the fiber's surface before and after different treatments. The observations on UTFD confirmed the presence of thorns on the epidermal layer attached to the UTFD outer surface. However, the inner surfaces, which are not covered by the epidermis, showed rough and smooth parts indicating the existence of remaining cells part as 'impurities'. The surface of TTFD seems to be clean. The NTFD showed a cleaner and rougher surface and a fibrillation could be noticed. Furthermore, the thorns had undergone a degradation. The STFD and ATFD also seems to have a cleaner surface than UTFD.

### Chemical composition

The proportion of the main components mass (lignin and carbohydrates, ash) of UTFD and the Diss leaves relative to the dry mass were identified and quantified. The results can be seen in Table 1 and Figure 6. Carbohydrates are the main components of Diss leaves and fibers with  $62,60 \pm 3,67\%$  and  $64,16 \pm 0,79\%$  of dry mass, respectively. The amount of lignin is also important: around 20% for both

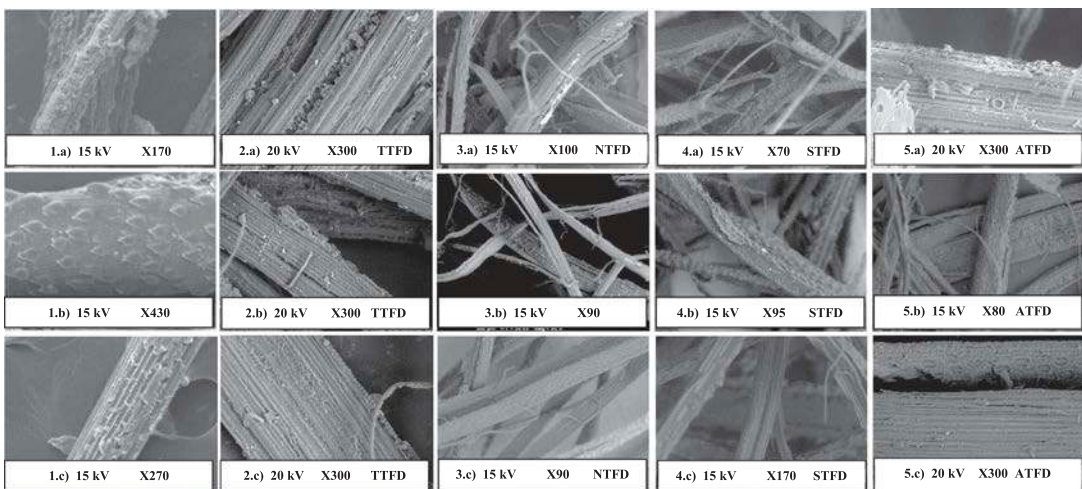
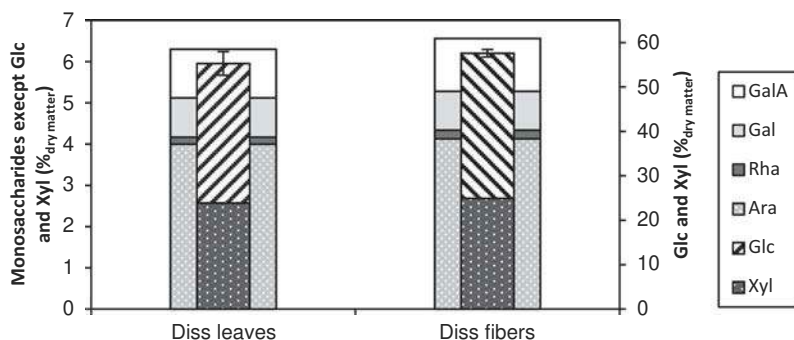


Figure 5. SEM observations of TFD surface: (1) untreated, (2) Heat treated at 140°C, (3) Treated with NaOH, (4) silane treated, (5) Treated with acetic acid.



**Table 1.** Chemical composition of leaves and fibers of Diss expressed as dry matter.

	Carbohydrates	Lignins	Ash	Total
Diss leaves (%)	61,60 ± 3.66	20.30 ± 0.30	4.41 ± 0.14	86.2
UTFD (%)	64,16 ± 0.79	20.66 ± 0.13	4.67 ± 0.12	89.7

**Figure 6.** Relative contents of monosaccharides in the leaves and fibers of Diss. Glc Glucose, GalA Galacturonic acid, Xyl xylose, Gal galactose, Rha rhamnose, Ara arabinose.

samples. The ash represents about  $4,50 \pm 0,17\%$  of the leaves and  $4,67 \pm 0,18\%$  of the fibers of Diss. From these results, we can see that there is not a significant change in the chemical composition of fibers and leaves.

Glucose and xylan are the main constituents of the carbohydrates present in the leaves and fibers of Diss with,  $31,41 \pm 2,65\%$ ,  $32,64 \pm 0,84\%$  and  $23,88 \pm 0,90\%$ ,  $24,95 \pm 0,12\%$  (Figure 6), respectively. These fibers could be classified as xylan-rich type fibers because of their important quantity of xylan (Bourmaud et al. 2018). These proportions are close to those of kapok, alfa and wood fibers (Bourmaud et al. 2018).

It was stated in the literature (Bledzki 1999; Bro et al. 2004; Pouzet 2012; Privas 2013; Sedan 2007;) that xylose and arabinose are present in the hemicellulose composition; Galactose is a component of pectin; Glucose is the predominant component of cellulose no less than it also enters the hemicellulose composition; Uronic acid and rhamnose are present in the composition of pectin and hemicellulose. This represents 29.09%, 0.94%, 32.64% and 1.49% relative to the dry mass of the diss fibers, respectively. These fibers are composed mainly of cellulose, hemicellulose and lignin with close proportions (between 20% to 35% in dry mass). However, the proportion of pectin should not exceed 2.50%. These proportions are close to those of kapok, alfa and wood fibers (Bourmaud et al. 2018).

## Spectroscopy

Figure 7a presents the different IR spectra of the untreated and treated fibers. The IR spectra of the NTFD showed changes in some peaks compared to that of the UTFD. It was found that the peaks  $2851 \text{ cm}^{-1}$ ,  $1740 \text{ cm}^{-1}$  and  $1462 \text{ cm}^{-1}$  disappeared. The peaks  $2851 \text{ cm}^{-1}$  and  $1740 \text{ cm}^{-1}$  correspond to the stretching vibrations of CH bonds of the methylene ( $\text{CH}_2$ ) and stretch-stretching groups of the C = O bonds, respectively, of lignin, hemicellulose and pectin. The peak  $1462 \text{ cm}^{-1}$  could be attributed to the vibrations of the hemicellulose aromatic bonds or lignin structure (Merkel et al. 2014). In addition, a significant decrease was observed for the peaks  $1513$  and  $1248 \text{ cm}^{-1}$  which were related to the stretching vibrations of the C = C, and C-O bonds of the aromatic rings and C = O bonds of the condensed units of guaiacyl lignin, respectively (Merkel et al. 2014). This could indicate significant removal of pectin and hemicellulose and less degradation of lignin from the surface of NTFD. These results are similar to those reported in the literature. However, the  $3600\text{--}3000 \text{ cm}^{-1}$  absorption band became wider and more intense after this treatment, the same remark can be raised for the peak  $897 \text{ cm}^{-1}$  against the intensity of



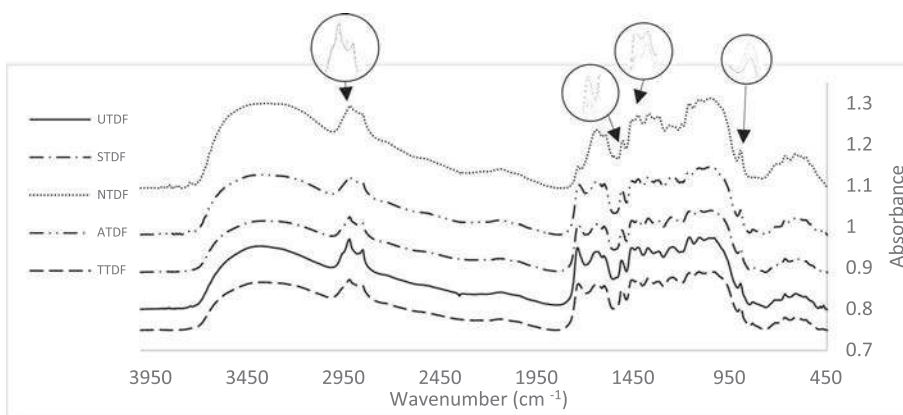


Figure 7. Infrared spectra of treated and untreated TFD.

this peak: The first band is attributed to the stretching vibration of the O-H bonds (Saravanakumar et al. 2014). The second peak corresponds to the  $\beta$ -glucoside binding of cellulose.

The fibers treated by silane, acetic acid and thermal treatment showed a decrease in peaks  $2920\text{ cm}^{-1}$ ,  $2856\text{ cm}^{-1}$  and  $1740\text{ cm}^{-1}$ . These peaks are related to the presence of lignin, pectin, and hemicellulose. For STFD, this could mainly be due to the ethanol/water solution in which the silane was mixed during the treatment. Hemicellulose and pectin have been reported to be partially eliminated in ethanol/water solution (Rachini et al. 2009; Zhou, Cheng, and Jiang 2014). However, The spectra showed an absence of silane peaks which should be present at  $766\text{ cm}^{-1}$  and  $847\text{ cm}^{-1}$  (Asim et al. 2016). It is possible that the amount of silane on the surface was so negligible that it has not been detected by FTIR (Sgriccia, Hawley, and Misra 2008). In the case of ATFD, these peaks ( $2920\text{ cm}^{-1}$ ,  $2856\text{ cm}^{-1}$  and  $1740\text{ cm}^{-1}$ ) could be related to the presence of waxy substances (Saravanakumar et al. 2014), which could indicate a degradation of these components. However, the absorption band  $3600\text{--}3000\text{ cm}^{-1}$  became less intense, this could be due to the interaction between  $\text{CH}_3\text{-CO-OH}$  and the  $\text{-OH}$  groups causing a decrease in the amount of the latter (Chung et al. 2018). It has been reported from the literature that IR spectra of acetylated plant fibers should show new peaks at  $1740\text{ cm}^{-1}$ ,  $1369\text{ cm}^{-1}$ ,  $1222\text{ cm}^{-1}$  (Chung et al. 2018) related to the stretching vibration of the (C = O) ester groups bonds, the bonds C- $\text{CH}_3$  and C-O of the acetyl groups, respectively. For the present work no significant changes were raised on these peaks. This could be explained by the fact that the quantity  $\text{CH}_3$  was not enough graft on the surface to be detected.

In the case of TTDF, these changes could be due to the partial degradation of some non-cellulosic unstable components in this temperature range such as lignin (Rong et al. 2001). The latter is slowly degraded over a wide temperature range of  $150\text{--}900^\circ\text{C}$  (Yang et al. 2007).

### Thermal stability

The thermal degradation of treated and untreated TFDs was studied by thermogravimetric analysis. The Table 2 shows the different peaks and percentages of mass losses associated with each stage of the pyrolysis determined by TG and DTG curves, respectively.

The DTG curve of UDF reached a peak at  $109^\circ\text{C}$  with a loss of mass of 9%, which could be attributed to moisture absorbed by the fibers (Rachini et al. 2009). Another more intense peak was observed at  $294^\circ\text{C}$ . The latter could correspond to the degradation of hemicellulose and pectin (Zhou, Cheng, and Jiang 2014), and the loss of mass due to this degradation is 27%. A last peak appeared at  $353^\circ\text{C}$  with a mass loss of 32%, which could be due to cellulose degradation (Yang et al. 2007). However, the degradation of lignin could be produced in the temperature range of  $150\text{ to }900^\circ\text{C}$  (Yang et al. 2007).

**Table 2.** TG and DTG results of treated and untreated Diss fibers.

	Pic (°C)	mass var (%)	Pic (°C)	mass var (%)	Pic (°C)	mass var (%)	rest
UTFD	109	8.8	294	26.6	353	32.2	32.4
TTFD	108	4.3	294	27.5	354	32.7	35.5
ATFD	123	7.5	326	21.9	372	34.3	36.3
STFD	124	8.4	319	25.0	373	35.5	31.1
NTFD	96	6.3	318	19.3	354	46.5	27.9

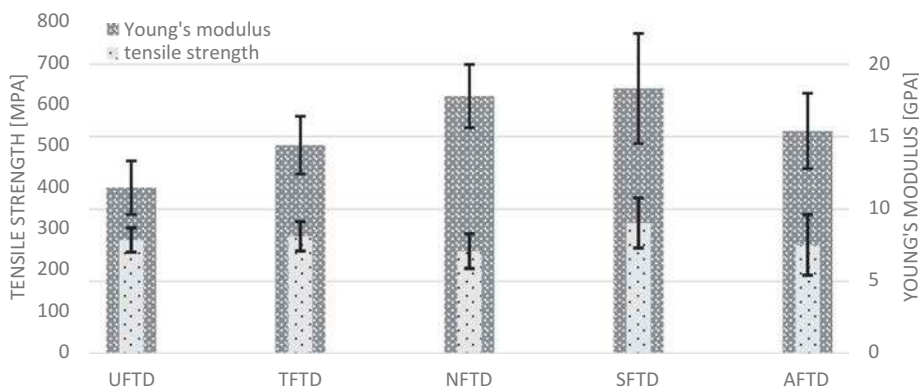
For the NTFD, the temperature of the second peak became higher (318°C) and the mass loss ratio significantly decreased (Table 2). This could be due to the partial degradation of hemicellulose and pectin after the alkaline treatment (Zhou, Cheng, and Jiang 2014). The mass loss corresponding to the cellulose degradation was remarkably higher compared to UTFD: 46.5%. This could be attributed to the increase of cellulose quantities after this treatment. For STFD and ATFD (Table 2), the three peaks that appeared in the DTG curve were shifted to higher temperatures. For the STFD, the thermal decomposition of the grafted silane is observed in the temperature range of 300–600°C (Rachini et al. 2009). This explains the improvement of the UTFD thermal stability: the silane grafted on the surface could play the role of a protective layer. For the ATFD, the same observations were made by Chung et al. (2018) on kenaf fibers. This improvement in thermal stability could be due to the CH<sub>3</sub>-CO-OH groups grafted onto the surface, which protects the Diss fibers components. Concerning TTFDs at 140°C (Table 2), a decrease was observed regarding the intensity of the first peak. This increase in UTFD hydrophobicity could be due to the degradation of certain hydrophilic components after this treatment, such as waxy substances.

### Tensile tests

Figure 8 shows the tensile stresses and Young's modulus of untreated and treated TFDs. The UTFD showed a tensile strength, a Young's modulus and an ultimate deformation, of  $273 \pm 36$  MPa,  $11.46 \pm 2.2$  GPa and  $2.6\% \pm 0.6$ , respectively. This resistance was the same magnitude order as for Kenaf fibers (Asim et al. 2016), Oil palm (Sreekala et al. 2000), pineapple leaves (Asim et al. 2016).

Bourahli and Osmani (2013) have found an average Young's modulus and tensile stresses of diss fibers of 8,7 GPa and 149 MPa, respectively. These results are close to those found by Bourahli (2018) where the average tensile stresses is 110 MPa, and a Young's modulus is 7.6 GPa. As a result, this extraction method better preserves the mechanical properties of the diss fibers.

After the various treatments, it was found that the average tensile stress significantly improved after the silane treatment with 15%. However, the tensile stress decreased after the alkaline treatment

**Figure 8.** Tensile stresses and young's modulus of untreated and treated TFDs, uncertainty (k = 2).

with -10%. In contrast, thermal and acetic acid treatments showed no significant change in the average tensile stress, respectively, with + 3% and -4%. Young's modulus significantly improved by an increase of 26%, 34%, 55% and 60% for respective different treatments: thermal, acetylation, alkaline and silane, respectively.

## Conclusion

This work aims to highlight the potential of the Diss fibers elements by assessing their use as reinforcement for polymer matrices (bio-composite). For that, Diss fibers were extracted by a manual method, which is based mainly on the morphology of this plant. After, these fibers have been treated with alkaline, silane, acetic acid and thermal treatments. The treated and untreated fibers underwent physicochemical characterizations to evaluate the effect of these treatments.

The untreated Diss fibers (UTFD) exhibited a low density of  $0.93 \text{ g/cm}^3$ , its chemical composition consisting mainly of glucose (32,6%), xylan (24.9%) and lignin (20.6%). UTFD exhibited a tensile strength, a Young's modulus, and an ultimate strain of  $273 \pm 36 \text{ MPa}$ ,  $11.4 \pm 2.2 \text{ GPa}$ , and  $2.67\% \pm 0.6$ , respectively.

Comparing to the UTFD, the chemical treated diss fibers showed a clean surface with a small diameter. In addition, the alkaline and silane treatments have significantly improved the stability of these fibers. Moreover, the acetic acid and silane treatments improved the Diss fiber thermal stability.

The Diss harbor interesting physicochemical characteristic that deserve to be test as a reinforcement in the polymer matrix.

## Acknowledgments

This research work has been conducted with the financial support of FEDER - Region Pays de la Loire in the framework of CIPTAP R&D project. Authors thank Camille Alvarado (INRA, BIA) for her skill and assistance in Acridine Orange microscopic preparation.

## Funding

This work was supported by the FEDER - Region Pays de la Loire.

## References

- Achour, A., F. Ghomari, and N. Belayachi. 2017. Properties of cementitious mortars reinforced with natural fibers. *Journal of Adhesion Science and Technology* 31:1938-62. doi:10.1080/01694243.2017.1290572.
- Ariawan, D., M. S. Salim, R. M. Taib, M. Z. A. Thirmizir, and Z. A. M. Ishak. 2018. Interfacial characterisation and mechanical properties of heat treated non-woven kenaf fibre and its reinforced composites. *Composite Interfaces* 25 (2):187-203. févr. doi:10.1080/09276440.2017.1354562.
- Asim, M., M. Jawaid, K. Abdan, and M. R. Ishak. 2016. Effect of Alkali and Silane treatments on mechanical and fibre-matrix bond strength of Kenaf and Pineapple leaf fibres. *Journal of Bionic Engineering* 13:426-35. doi:10.1016/S1672-6529(16)60315-3
- Baley, C. 2013. Fibres naturelles de renfort pour matériaux composites. AM5130 V2. *Techniques de l'Ingénieur*. Saint-Denis. France. [www.techniques-ingenieur.fr/base-documentaire/materiaux-th11/materiaux-composites-presenta-tion-et-renforts-42142210/fibres-naturelles-de-renfort-pour-materiaux-composites-am5130/](http://www.techniques-ingenieur.fr/base-documentaire/materiaux-th11/materiaux-composites-presenta-tion-et-renforts-42142210/fibres-naturelles-de-renfort-pour-materiaux-composites-am5130/)
- Blakeney, B., P. Harris, and R. Henry. 1983. A simple and rapid preparation of alditol acetates for monosaccharide analysis. *Carbohydrate Research* 113:291-99. doi:10.1016/0008-6215(83)88244-5.
- Bledzki, A. 1999. Composites reinforced with cellulose based fibres. *Progress in Polymer Science* 24 (2):221-274. doi:10.1016/S0079-6700(98)00018-5.
- Bourahli, M. E. H. 2014. *Caractérisation d'un composite verre/époxy*. Sciences. Algeria: Université Ferhat Abbas Setif 1.
- Bourahli, M. E. H. 2018. Uni- and bimodal Weibull distribution for analyzing the tensile strength of Diss fibers. *Journal of Natural Fibers* 15:843-52. doi:10.1080/15440478.2017.1371094.
- Bourahli, M. E. H., and H. Osmani. 2013. Chemical and mechanical properties of Diss (*Ampelodesmos mauritanicus*) fibers. *Journal of Natural Fibers* 10:219-32. doi:10.1080/15440478.2012.761115.

- Bourmaud, A., J. Beaugrand, D. U. Shah, V. Placet, and C. Baley. 2018. Towards the design of high-performance plant fibre composites. *Progress in Materials Science* 97:347–408. doi:10.1016/j.pmatsci.2018.05.005.
- Bro, J., J. Harholt, H. V. Scheller, and C. Orfila. 2004. Rhamnogalacturonan I in *Solanum tuberosum* tubers contains complex arabinogalactan structures. *Phytochemistry* 65:1429–38. doi:10.1016/j.phytochem.2004.05.002.
- Chilali, A. 2017. Étude expérimentale et modélisation de la durabilité des biocomposites à fibres de lin. Thèse, Mécanique. Université de Reims Champagne-Ardenne.
- Chung, T.-J., J.-W. Park, H.-J. Lee, H.-J. Kwon, H.-J. Kim, Y.-K. Lee, and W. Tai Yin Tze. 2018. The improvement of mechanical properties, thermal stability, and water absorption resistance of an eco-friendly PLA/Kenaf biocomposite using acetylation. *Applied Sciences* 8:376. doi:10.3390/app8030376.
- Damerdj, A. 2012. Les Orthoptéroïdes sur différentes plantes dans la région de Tlemcen (Algérie). *Afrique SCIENCE* 8:82–92.
- Dixon, W. J. 1953. Processing data for outliers. *Biometrics* 9:74–89. doi:10.2307/3001634.
- Haque, R., M. Saxena, S. C. Shit, and P. Asokan. 2015. Fibre-matrix adhesion and properties evaluation of sisal polymer composite. *Fibers Polymer* 16 (1):146–52. janv. doi:10.1007/s12221-015-0146-2.
- Hatfield, R., and R. S. Fukushima. 2005. Can lignin be accurately measured? *Crop Science* 45:832–39. doi:10.2135/cropsci2004.0238.
- Hu, W., M.-T. Ton-That, F. Perrin-Sarazin, and J. Denault. 2010. An improved method for single fiber tensile test of natural fibers. *Polymer Engineering & Science* 50:819–25. doi:10.1002/pen.21593.
- Merkel, K., H. Rydarowski, J. Kazimierzak, and A. Bloda. 2014. Processing and characterization of reinforced polyethylene composites made with lignocellulosic fibres isolated from waste plant biomass such as hemp. *Composites Part B: Engineering* 67:138–44. doi:10.1016/j.compositesb.2014.06.007.
- Merzoud, M., and M. F. Habita. 2008. Elaboration de composite cimentaire à base de diss « *Ampelodesma Mauritanica* ». *Afrique Science: Revue Internationale Des Sciences Et Technologie* 4 (2):231–45.
- Methacanon, P., U. Weerawatsophon, N. Sumransin, C. Praharn, and D. T. Bergado. 2010. Properties and potential application of the selected natural fibers as limited life geotextiles. *Carbohydrate Polymers* 82:1090–96. doi:10.1016/j.carbpol.2010.06.036.
- Pouzet, D. 2012. *Production durable de biomasse: La lignocellulose des poacées*. France: Quae.
- Privas, E. 2013. Matériaux ligno-cellulosiques: «*Élaboration et caractérisation* ». Ecole Nationale Supérieure des Mines de Paris
- Rachini, A., M. L. Troedec, C. Peyratout, and A. Smith. 2009. Comparison of the thermal degradation of natural, alkali-treated and silane-treated hemp fibers under air and an inert atmosphere. *Journal of Applied Polymer Science* 112:226–34. doi:10.1002/app.v112:1.
- Rameau, J.-C., D. Mansion, and G. Dumé. 1989. *Flore forestière française: Guide écologique illustré Région méditerranéenne* [French forest flora: Illustrated ecological guide Mediterranean region]. 3rd ed. Paris: AgroParis Tech-ENGREF.
- Rong, M. Z., M. Q. Zhang, Y. Liu, G. C. Yang, and H. M. Zeng. 2001. The effect of fiber treatment on the mechanical properties of unidirectional sisal-reinforced epoxy composites. *Composites Science and Technology* 61:1437–47. doi:10.1016/S0266-3538(01)00046-X.
- Sarasini, F., J. Tirillò, G. Maffei, A. Zuorro, R. Lavecchia, F. Luzi, D. Puglia, L. Torre, and A. Maghchiche. 2019. Thermal and mechanical behavior of thermoplastic composites reinforced with fibers enzymatically extracted from *Ampelodesmos mauritanicus*. *Polymer Engineering & Science*. doi:10.1002/pen.25093.
- Saravanakumar, S. S., A. Kumaravel, T. Nagarajan, and I. G. Moorthy. 2014. Investigation of physico-chemical properties of Alkali-treated prosopis juliflora fibers. *International Journal of Polymer Analysis and Characterization* 19:309–17. doi:10.1080/1023666X.2014.902527.
- Sedan, D. 2007. *Etude des interactions physico-chimiques aux interfaces fibres de chanvre/ciment : Influence sur les propriétés mécaniques du composite*. Université de Limoges.
- Sgriccia, N., M. C. Hawley, and M. Misra. 2008. Characterization of natural fiber surfaces and natural fiber composites. *Composites Part A: Applied Science and Manufacturing* 39:1632–37. doi:10.1016/j.compositesa.2008.07.007.
- Sreekala, M. S., M. G. Kumaran, S. Joseph, M. Jacob, and S. Thomas. 2000. Oil palm fibre reinforced phenol formaldehyde composites: Influence of fibre surface modifications on the mechanical performance. *Applied Composite Materials* 7:295–329. doi:10.1023/A:1026534006291.
- Thibault, J. 1979. Automatisation du dosage des substances pectiques par la méthode au méthahydroxydiphényle. *Lebensmittel-Wissenschaft Und Technologie* 12:247–51.
- Yang, H., R. Yan, H. Chen, D. H. Lee, and C. Zheng. 2007. Characteristics of hemicellulose, cellulose and lignin pyrolysis. *Fuel* 86:1781–88. doi:10.1016/j.fuel.2006.12.013.
- Zhou, F., G. Cheng, and B. Jiang. 2014. Effect of silane treatment on microstructure of sisal fibers. *Applied Surface Science* 292:806–12. doi:10.1016/j.apsusc.2013.12.054.